Snapshot GNSS receivers for low-effort, high-gain space situational awareness

Gill, E.; Akos, D. M.

DOI
10.1016/j.asr.2023.11.041

Publication date
2024

Document Version
Final published version

Published in
Advances in Space Research

Available online at www.sciencedirect.com

ScienceDirect

Advances in Space Research 73 (2024) 42–52

ADVANCES IN SPACE RESEARCH (a COSPAR publication)

www.elsevier.com/locate/asr

Snapshot GNSS receivers for low-effort, high-gain space situational awareness

E. Gill [a,*], D.M. Akos [b]

[a] Space System Engineering, Delft University of Technology, Kluyverweg 1, 2629HS, Delft, The Netherlands
[b] Aerospace Engineering Sciences, University of Colorado, 3775 Discovery Dr., Boulder, CO 80303, United States

Received 17 August 2023; received in revised form 24 November 2023; accepted 26 November 2023
Available online 29 November 2023

Abstract

This paper proposes a novel concept of using highly efficient Snapshot Global Navigation Satellite Systems (GNSS) receivers to provide precise position fixes of single or multiple satellites in Low-Earth Orbit (LEO) to improve upper atmospheric modeling and thus contribute to superior space situational awareness (SSA). While tracking of LEO satellites and the use of onboard GNSS receivers for drag measurements and upper atmosphere modeling are well-established techniques, the expected advent of snapshot GNSS receivers for spaceborne scientific applications will allow massive improvements on the GNSS sensor's Size, Weight, Power and Cost (SWaP-C). With chip-size dimensions of 4x4 mm^2, a mass of less than 5 gr, an average power level below 0.1 mW, snapshot receiver technology is expected to provide position fixes in space with an accuracy of ~19 m (3D r.m.s.), which will surpass the accuracy of Two-Line Elements (TLE) provided by the US Joint Space Operations Center (JSpOC) by at least two orders of magnitude. Equally important to their SWaP-C benefits, Snapshot GNSS receivers will allow mission and spacecraft designers to trade onboard-processing requirements versus payload downlink requirements, leading to either minimum onboard processing or a minimum amount of downlinked data. In this research, we establish the concept and architectural overview of using snapshot GNSS receivers for SSA, including the role of using them in a Distributed Space System (DSS), and detail their characterization and performance in terms of the required GNSS hardware and the impact of these payload on the power budget, the link budget and the OnBoard Data Handling (OBDH) budget of a satellite. It will be shown that these receivers lend themselves especially to their use on femto-, pico- and nano-satellites, although integrated snapshot modules may be flown as auxiliary payloads on micro- or mini-satellites as well. While this work focuses on the implications of the use of snapshot GNSS receivers on spacecraft design for the use of upper atmosphere modeling and SSA, their use may open up other science applications which avoid the need for expensive high-grade GNSS receivers.

Keywords: GNSS receiver; Snapshot receiver; Atmospheric drag; Upper atmosphere density modeling; Space Situational Awareness

1. Introduction

1.1. Context and need

The increasing number of objects in space, whether debris, left upper rocket stages, and de-functional or functional satellites, poses a growing risk for existing space infrastructure and its services. Space Situational Awareness (SSA), the knowledge and characterization of space objects and their operational environment, is an important area to understand, characterize and manage those threats. Within SSA, the space surveillance and tracking (SST) segment is key to contribute to increased SSA. An element to provide such tracking functions is e.g. the Space Surveillance Network of the U.S. Strategic Command (USSTRATCOM), which enables the maintenance of a Space Object Catalog

* Corresponding author.
E-mail addresses: e.k.a.gill@tudelft.nl (E. Gill), dma@colorado.edu (D.M. Akos).

https://doi.org/10.1016/j.asr.2023.11.041
0273-1177/

(USSTRATCOM, 2023), provided to the public in the form of so-called Two-Line Elements (TLEs) per object and updated at least once daily. While tracking of space objects enables the localization of these objects at specific epoch, the crucial SST function is, however, its orbit prediction capabilities, i.e. the knowledge of the positions of these objects in the future for applications, such as collision avoidance. This requires, apart from relevant tracking data, a reliable modeling of the dynamics of these objects. While these models, comprising gravitational and non-gravitational forces, are in general well developed and understood (Montenbruck and Gill, 2001), the largest contribution of non-gravitational forces for objects in LEO below 750 km stems from atmospheric drag. Atmospheric drag reduces the energy from the orbit and causes a decrease in the orbital period and eccentricity over time (King-Hele, 1987). The largest factor of uncertainty for modeling of atmospheric drag is the thermosphere neutral density, which is computed using empirical thermospheric density models, which show RMS errors of up to 30 % and peak errors of some 100 % (Marcos et al., 2006).

The objective of this paper is to contribute to the improvement of empirical thermospheric density models, both in terms of increased accuracy and reduced latency, through the use of so-called snapshot Global Navigation Satellite Systems (GNSS) receivers, which provide, when flown on LEO satellites, position fixes at extremely low Size, Weight, Power and Cost (SWaP-C). Through the future use of these spaceborne GNSS data, originating from multiple satellites, increased accuracy and reduced latency of empirical thermospheric density models can be achieved, which will in turn improve orbit prediction capabilities and thus contribute to an improved SSA.

1.2. State-of-the-Art

Modeling the thermospheric density is extremely challenging, as the density shows, apart from a prominent decrease with increasing altitude, complex daily, seasonal, and latitudinal dependencies and thus depends on time, date and location. Moreover, solar and geomagnetic activities strongly impact the thermospheric density, leading to the use of proxies and indices in the empirical density models, such as the observed 10-cm solar flux $F_{10.7}$, and the planetary geomagnetic indices K_p or a_p. For orbit prediction, empirical models such as Jacchia-1972 (Jacchia, 1979), DTM-2012 (Bruinsma et al., 2003) and NLRMSIS-00 (Picone et al., 2002) are used. The largest factor of uncertainty in the thermosphere neutral density is the lack of accurate density measurements with good spatial and temporal resolution (Kuang et al., 2014).

There are three approaches to generate measurements and data, which can contribute to improved thermospheric density models. First, in-situ measurements of atmospheric composition, cross-track winds and neutral temperature are collected from dedicated satellite missions, such as the Atmospheric Neutral Density Experiment (ANDE) of the U.S. Naval Research Laboratory with a Wind And Temperature Spectrometer (WATS) (Nicholas et al., 2003). Although these data provide high-temporal resolution during specific measurement arcs, they do neither provide a global coverage, nor are they collected in an operational manner over continuous long arcs of years. Also, these data do not reflect the actual impact of the thermospheric density on atmospheric drag, experienced by space objects.

Second, there are dedicated satellite missions, typically high-end multi-purpose geodetic missions, which provide direct measurements of the accelerations experienced by these satellites. Examples of these missions are the Challenging Minisatellite Payload (CHAMP) (Reigber et al., 2002, Moore et al., 2003), the Gravity Recovery and Climate Experiment (GRACE) (Tapley et al., 2004, van den Ijssel and Visser, 2007) and GRACE Follow-on (Landerer et al., 2020, Behzadpour et al., 2021), the Gravity Field and Steady-State Ocean Circulation Explorer (GOCE) (Rummel et al., 2011, Visser and van den Ijssel, 2016) and the SWARM mission (Friis-Christensen et al., 2008, Siemes et al., 2016). In many cases, the accelerometer measurements need to be processed with accompanying GNSS data to be able to separate accelerations from atmospheric drag from other accelerations, acting on the spacecraft, such as solar radiation pressure and spacecraft attitude maneuvers. Moreover, the calibration and validation of accelerometer data can be rather complex, as in the case of GOCE (Visser and van den Ijssel, 2016), or suffer from a variety of disturbances, such as slow temperature-induced bias variations and sudden bias changes in the case of SWARM (Siemes et al., 2016). These difficulties have led to alternative approaches, which even completely discard accelerometer data in favor of processing the available GPS data (van den Ijssel et al., 2020).

Third, tracking of space objects and orbit determination of satellites provides position and velocity information, which can be used to infer information on acceleration, including and in particular the atmospheric drag as the largest and most uncertain contributions of all acceleration sources, and thus information on the thermospheric neutral density. While the effect of altitude decay is most notable during the reentry phase of missions, such as for GOCE (Cicalo et al., 2017), systematic differences in modeled trajectories and measured positions for many space objects in LEO can, when applying the necessary scientific rigor, often be associated to unmodelled atmospheric drag effects. The measurements, from which the trajectories are derived, can be ground-based, such as radar data, radiometric range and Doppler measurements, Satellite Laser Ranging (SLR), from Doppler Orbitography and Radiopositioning Integrated by Satellite (DORIS) (Willis et al., 2005), or spaceborne, typically generated by GNSS receivers onboard the satellites. Radar measurements to thousands of space objects are used by the Space Surveillance Network of the U.S. Strategic Command (USSTRATCOM), which enables the maintenance of a Space Object Catalog

(USSTRATCOM, 2023) to provide the so-called TLEs containing orbit information per object with a position accuracy of about 1 km (Aida et al., 2009) which allow a temporal resolution for atmospheric density of 3 days or longer (Doornbos et al., 2008). In contrast, traditional ground-based radiometric range and Doppler measurements allow position accuracies of LEO satellites of about 10 m (Montenbruck and Gill, 2001), while SLR provides a 3D position accuracy of a few centimeters for satellites which are equipped with laser retroreflector arrays (LRAs) (Arnold et al., 2019). While TLEs are characterized by low accuracy and low temporal resolution, available on a continuous basis, other ground-based tracking methods provide moderate or precise position information, limited to specific tracking arcs and a small number of satellites, which typically would allow the reconstruction of atmospheric density only on time scales of days. Spaceborne tracking of LEO satellites using GNSS receivers is a common technique to support satellite, payload and ground station operations (Teunissen and Montenbruck, 2017). Specific geodetic-type of missions employing high-grade multi-frequency receivers, such as with CHAMP, GRACE, GRACE Follow-On, GOCE and SWARM are using the GNSS raw pseudo-range and carrier phase data, and combinations thereof, to infer thermosphere neutral density from these data (van den Ijssel et al., 2020). However, this approach is neither suitable to provide global coverage nor does it provide continuous timely information about the thermospheric neutral density of the upper atmosphere. Last, but not least, the high-grade spaceborne receivers have been specifically designed, produced and validated for space applications, leading to very costly systems with high SWaP-C values on very expensive missions. An example of such a receiver is the TriG by Moog Broad Reach with a form factor of $19 \times 22 \times 12$ cm^3, a mass of 6 kg and 55 W of power consumption (Teunissen and Montenbruck, 2017). An overview of spaceborne GNSS receivers with their SWaP values used on previous missions, including many high-grade geodetic GNSS receivers on science missions, is provided in (Gill et al., 2023). The BlackJack receiver onboard the CHAMP satellite with a mass of 3.2 kg and a power consumption of 15 W (Gill et al., 2023) delivered RMS values of phase residuals at sub-centimeter level and enabled orbit reconstructions with position accuracies of several centimeters and empirical accelerations of several nm/s^2 (Moore et al., 2003).

In contrast to standard space-capable or high-grade geodetic GNSS receivers, snapshot receivers provide extremely low SWaP-C and thus offer a more efficient approach to position estimation than traditional GNSS positioning methods. In contrast to traditional GNSS receivers, snapshot receivers sleep for most of the time and wake up at defined intervals to record short snapshots of GNSS signals. These receivers digitize the raw signals and store them locally, while the processing of these signals and the execution of the estimation algorithms is done on separate processors. Also in contrast to traditional receivers, the estimation of position from signal snapshots is too short to decode signal transmission timestamps or information about the GNSS satellite positions. Thus, this information has to be provided from public sources. However, the timestamps have to be reconstructed from the raw snapshot. An example of such a snapshot receiver is the SnapperGPS (Beuchert and Rogers, 2021), with a form factor of $3 \times 3 \times 1$ cm^3 (est.), a mass of 0.003 kg (est.) and a power consumption of 12.6 mAh per year. The use of a snapshot receiver in space is not new. In fact, as part of the "Falcon Gold" experiment, a hosted payload comprising a NAVSYS TIDGET sensor attached to a Centaur upper stage collected in November 1997 data from signal acquisition of GPS satellites (Powell et al., 1999) in a snapshot mode. In February 1998, the microGPS receiver started to collect snapshots for navigation purposes onboard of the SNOE mini-satellite (Srinivasan et al., 2000). However, since this time no other snapshot receivers have, to the best knowledge of the authors, been flown in space. Moreover, in this paper, a spaceborne snapshot GNSS receiver is proposed for the first time for science applications.

1.3. Innovation and organization

The innovation of this paper comes from the fact that Snapshot GNSS receivers flown on one or several satellites will provide position fixes for scientific purposes, such as thermospheric neutral density estimations, at extremely low SWaP-C values, while offering the flexibility of adapting the frequency of snapshots to the user needs. It is, to the best knowledge of the authors, the first time, that snapshot GNSS receivers are proposed for spaceborne science applications. The accuracy of the position fixes is expected to be better than 15 m (Beuchert and Rogers, 2021) and thus around two orders of magnitude superior to what is provided by TLEs. In addition to the low SWaP-C values, the designer of the payload and satellite system obtains the choice of processing the snapshots onboard and thus have extremely low downlink needs of several Bytes per snapshot, or of saving snapshot processing power onboard in expense for a higher bandwidth for payload telemetry. Thus, the proposed concept closes the gap between the limitations of TLE-based global coverage, high-latency, high-latency approaches and the very costly, GNSS-based high-accuracy, limited coverage, but low-latency concepts.

Section 2 introduces the concept of GNSS Snapshot-based thermosperhic neutral density estimation, the architectural overview and the impact of using such systems on several satellites. Section 3 provides the detailed system characterization and the performance analysis in terms of satellite system design. Section 4 sketches the roadmap towards an implementation of such system including a discussion of critical challenges to be overcome. Section 5 summaries the main contributions and findings of this work and provides an outlook.

2. Concept and architectural overview

2.1. Concept of drag and density estimation

A snapshot GNSS receiver will typically provide position fixes at a user-defined frequency. The accuracy of such fixes is expected to be better than 15 m (Beuchert and Rogers, 2021) and will, if the receiver is properly configured for space scenarios, not be deteriorated for space applications, as compared to terrestrial applications. The characteristic time scales at which drag and density variations appear relevant to improve density models are hours. Thus, an hourly rate of position fixes is used as an assumption in the sequel for the configuration of snapshot receivers. Such temporal resolution is better by at least a factor of ~3 * 24 than what USSTRATCOM's TLEs provide (Doornbos et al., 2008). Moreover, the temporal resolution is flexible, as the data rate can be adjusted by the user.

The estimation of the acceleration from atmospheric drag and inference of neutral density is based on the fundamental relation (Montenbruck and Gill, 2001)

$$\ddot{\boldsymbol{r}} = -\frac{1}{2} C_D \frac{A}{m} \rho v_r^2 \boldsymbol{e}_v \tag{1}$$

where the drag coefficient C_D is a dimensionless quantity that describes the interaction of the atmosphere with the satellite's surface material, A is the satellite's cross-sectional area, m the mass of the satellite, ρ the atmospheric density at the location of the satellite, and v_r the velocity of the object relative to the atmosphere. The direction of the drag acceleration is always (anti-)parallel to the relative velocity vector as indicated by the unit vector $\boldsymbol{e}_v = \boldsymbol{v}_r/v_r$.

A fundamental problem of estimating atmospheric densities from satellite accelerations or its double-integrated quantities of positions, is that density is correlated to the quantities v_r, C_D, A and m as shown in Eq. (1). While the velocity of the object relative to an assumed co-rotating atmosphere is very well known, wind models should be accounted for, certainly for precision applications. In addition, full correlation of the density exists with the so-called ballistic coefficient $B = C_D\,(A/m)$. The cross-sectional area A of the satellite may change over time due to attitude maneuvers and thus would require continuous attitude knowledge or the use of dedicated spherical satellites, such as ANDE (Nicholas et al., 2003), DANDE (Pilinski and Palo, 2009) or Q-Sat (Zhao et al., 2019). Also, the mass of the satellite may change due to propulsion activities. However, in many cases in practise, the ratio of A/m is assumed to be known and constant, when estimating densities. The most challenging correlation of the density is, however, with the drag coefficient drag coefficient C_D, as this coefficient depends on various factors, such as the geometrical space of the body, the materials of the body as well as the chemical composition of the upper atmosphere and its temperature. Various strategies are available to cope with the uncertainties of the drag and/or ballistic coefficients and to decouple them from the thermosphere density, such as modelling using spacecraft geometry, statistical means, such as assuming that the long-term average of the ratio of observed over modelled density ratios should equal one (Doornbos et al., 2008), or reference satellites, where these parameters are better known (Granholm et al., 2002). Another strategy is to make assumptions on the long-term behaviour of these coefficients, which could then be treated by estimating e.g. daily drag coefficients as part of the state vector in orbit determination algorithms. This would then decouple these coefficients from empirical accelerations, being attributed to density variations, which are estimated every e.g. 5 min (Kuang et al., 2014).

One of the first, and still widespread, approaches to derive densities from tracking, is based on (King-Hele, 1987) which applies an analytic model, a very coarse atmospheric model, including a priori information such as the atmospheric density scale height parameter, to determine neutral density values from position estimates of satellites. However, this model assumes that the Earth's gravitational perturbations have a negligible long-term influence on the osculating semimajor axis of an object on LEO orbit. In addition, as his model is based on osculating elements, care must be taken when applying TLEs to his approach, as the TLEs are based on the SGP4 model (Hoots & Roehrich, 1980), which deliver mean orbital elements.

Specifically for deriving density values from TLEs, (Picone et al., 2005) have developed an efficient algorithm, which generates integrated thermospheric mass density values from the mean of mean motion values, weighted by the instantaneous velocity and wind correction factors, calculated along that trajectory. While their approach is independent on any thermospheric model, the results still depend on the ballistic coefficient. In a test campaign with TLEs from 50 satellites, (Doornbos et al., 2008) were able to show that using only a single calibration factor per day already improves the RMS of daily integrated densities along the orbit from a level of around 30 % to below 16 %. The ability to correct empirical model densities using TLEs of Cubesats during geomagnetic storms was demonstrated by (Brandt et al., 2020).

The tracking of LEO objects using GPS receivers provides position information that can be treated similar to TLEs to retrieve neutral density data and thus improve thermosphere models. Alternatively, it can augment satellite acceleration measurements or even replace them (van den Ijssel et al., 2020) for the same purpose. The principle has been analyzed in (van den Ijssel and Visser, 2007) for the CHAMP and GRACE satellites. Here, especially the along-track components, being dominant for atmospheric drag, could be well observed, while the cross-track component was less prominent and the radial component did not provide clear signals. Total atmospheric density has been derived by determining the drag force acting on the four satellites, CHAMP, GRACE, SAC-C, and TerraSAR-X through centimeter-level reduced dynamic precise orbit determination (POD) by (Kuang et al., 2014). They were able to show that the along-track GPS-derived

acceleration for these satellites allowed a precision of 2 nm/s^2, about 3 % of the total acceleration due to drag at 500 km altitude. Above 715 km altitude, they found that their 5-minute temporal resolution would no longer provide useful information.

Inspired by Kuang et al. (2014) and based on dynamical considerations, it is possible to derive a relation between the standard deviation of the theoretical relative density error $\sigma_{\rho,rel}$ as a function of the spacecraft altitude h for various values of temporal resolution τ. This theoretical relative density error can be written as

$$\sigma_{\rho,rel}(h) \cong 2\frac{\sigma_{pos}}{\tau^2\rho(h)} \tag{2}$$

where ρ denotes the atmospheric density and σ_{pos} the standard deviation of the 3D position error. This relation is shown in Fig. 1. The atmospheric density values have been computed based on the Harris–Priester atmospheric density coefficients valid for mean solar activity (Montenbruck and Gill, 2001).

It is obvious that the relative density error rapidly increases with increasing altitude, as the perturbations from atmospheric drag exponentially decrease for increasing altitude. They are thus no longer detectable given a specific position measurement error. Values of the relative density error above 30 % are typically useless, unless there is high solar or geomagnetic activity. While a temporal resolution of one orbital period is, for single satellites, not competitive with TLE or POD methods (using $\sigma_{pos,TLE} =$ 1 km, $\tau_{TLE} = 3$ d and $\sigma_{pos,POD} = 1$ mm, $\tau_{POD} = 5$ min, respectively), it is found that using snapshot GNSS receivers with time resolutions of 8 h provide very comparable results to the TLE or POD methods.

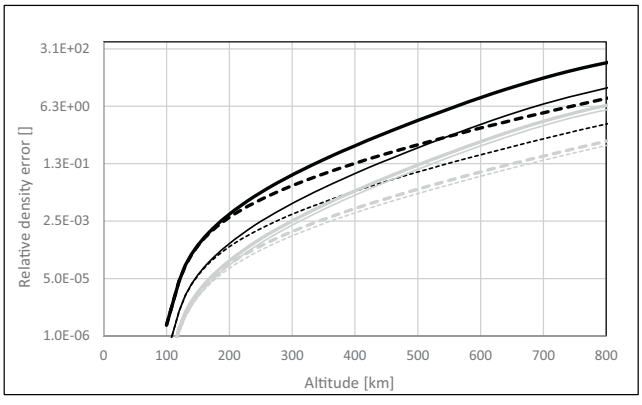

Fig. 1. Relative density reconstruction error (black lines) as a function of spacecraft altitude for snapshot GNSS receivers ($\sigma_{pos} = 10$ m). Solid lines refer to minimum mean density and dashed lines to maximum mean density for mean solar activity (Montenbruck and Gill, 2001). Black thick lines refer to a sampling time of one orbital period and black thin lines to a sampling time of 4 h. Thick grey lines refer to the case of TLEs. Thin grey lines refer to the case of POD results.

2.2. The role of a distributed space architecture

Although focused on single satellites, (Kuang et al., 2014) noticed that errors in measured atmospheric density can be averaged down when combined from multiple satellites over multiple years for parameters associated with atmospheric density. While USSTRATCOM with its space objects catalogue provides an excellent basis in terms of the number of available objects, the TLEs' position accuracies and temporal resolutions are main obstacles to improve atmospheric models in an operational manner. In contrast, POD methods using high-grade GNSS receivers on selected science satellites provide high accuracy, high temporal resolution data to improve atmospheric density models. However, only few large and expensive satellites are available with such equipment.

Thus, a suitable space architecture with distributed snapshot GNSS receivers would provide an opportunity to fill this gap between TLE and POD by offering position fixes with reasonable accuracy and adjustable temporal resolution at very low SWaP-C values. Snapshot GNSS receivers may be used on several to many dedicated femto- or pico-satellites, or be part of the payload suite for nano-, micro- or mini-satellites, to improve atmospheric density models further. To provide an optimal global coverage, the distribution of these satellites in LEO should show variations in inclination, local time of the ascending node, possible eccentricity and cover an altitude regime of 200–600 km. Due to the low SWaP-C, dedicated low-cost femto- and pico-satellites can be considered in particular for Very Low Earth Orbits (VLEO) with altitudes well below the International Space Station (ISS). While this implies short lifetimes, the efforts to implement such missions are, except for launch, low and guarantee a sustainable solution in terms of the low risk, they pose to other operational missions and to generate orbital debris.

A methodology to generate near-real-time atmospheric density correction using multiple satellites, which will be usable for satellites equipped with GNSS snapshot receivers, has been described in (Granholm et al., 2002). They use a set of satellites, which they distribute in standard satellites which well-known ballistic coefficients (1/10 of the total object population being effective) and a larger part of non-standard satellites with assumed ballistic coefficients that are neither constant nor well known. In an iterative process, they associate ballistic correction factors for non-standard satellites to density variations which can inform atmospheric model updates. Generalizing their statistical analysis, the standard deviation of the residual errors on the ballistic coefficients, and thus on density corrections $\sigma_{\Delta\rho}$, is

$$\sigma_{\Delta\rho} = \frac{\sqrt{\sum_{i\in N}\Delta_i^2}}{\sqrt{N}} \tag{3}$$

where N denotes the total number of satellites in the sample and Δ_i denotes the residual error for the density correction estimation for satellite i. Thus, the relative density error does not only increase with increasing altitude, as shown in Fig. 1, but also decreases with an increasing number of satellites carrying GNSS snapshot receivers. This dependency of density reconstruction errors from GNSS snapshot receivers parametrized by the total number of satellites, combining (2) and (3), is shown in Fig. 2.

2.3. Concept of operations

Fig. 3 shows a simplified version of the concept of operations for providing updated services to users based on snapshot GNSS receivers. The space segment consists of two parts. It makes use of the GNSS satellites of the GPS, Galileo, GLONASS, and BeiDou satellites at Medium Earth Orbit (MEO). The second part of the space segment comprises a number of satellites in LEO, which constitute a diverse Distributed Space Systems (DSS), which itself may comprise satellites flying in formation or a swarm or a constellation of satellites. This DSS system is diverse and flexible as it may comprise various satellite operators, as indicated in Fig. 3. Moreover, the snapshot GNSS receivers may be flown as single payload on dedicated satellites, or as secondary payload on general-purpose satellites or even as hosted payloads on other satellites.

The ground segment comprises again two parts. First, there are various numbers of satellite operators with their respective satellite ground control centers (GCC) and ground station complexes. Those GCCs provide the relevant data from the various snapshot receivers further to the Processing Center, the second part of the ground segment, which executes the algorithms, e.g. referenced in Section 2, and generates products, such as updated parameters for atmospheric density modeling to the users. This service

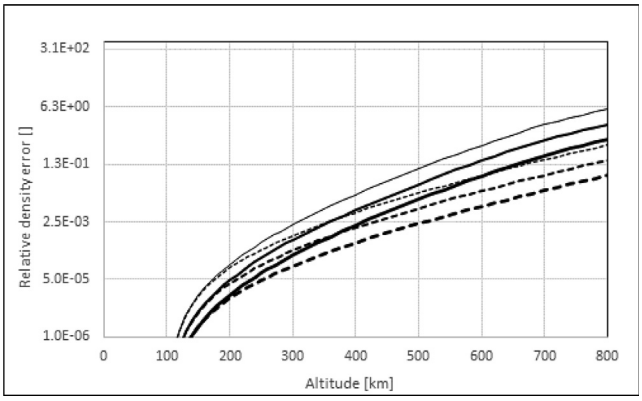

Fig. 2. Relative density reconstruction error as a function of spacecraft altitude for multiple snapshot GNSS receivers ($\sigma_{pos} = 10$ m, sampling time of 8 h). Solid lines refer to minimum mean density and dashed lines to maximum mean density for mean solar activity (Montenbruck and Gill, 2001). Thin, medium and thick lines refer to $N = 1$, $N = 8$, and $N = 64$ satellites, respectively.

can be operated offline or in near real time, depending on the user needs and the system constraints. The Processing Center can be realized at universities, research institutes, companies, space agencies or governmental institutions.

2.4. Onboard GNSS system architecture

A traditional GNSS receiver is comprised of three functionalities. First, signal capture will collect digital samples of the incoming Radio Frequency (RF) signals. Second, signal processing will acquire those satellites that are trackable and will output raw measurements, such as pseudorange (PR), Doppler frequency and carrier phase (CP). Third, position estimation will compute a position and velocity using the PR, Doppler and possibly CP measurements.

In contrast, snapshot positioning uses only a very brief time interval of the received satellite signal with sampling times of some 100 milliseconds (ms) to even down to as little as 2 ms. Most of the time, snapshot receivers are in deep sleep and only wake up during user-specified intervals, such as hours (Wang et al., 2019). Thus, they are ideally suited for energy-limited applications, such as asset tracking, fleet management, wildlife tracking, geofencing, incidence reporting and Internet of Things (IoT) applications. For this reason, snapshot receivers are a very promising technology for small satellites as well, where power is, together with form factor and mass, a key limiting resource.

Moreover, the fact that snapshot receivers store the complete digital samples during signal capturing, though over a rather short time window, means that the digital samples can either be used in real time or later for signal processing. Similarly, after signal processing, position estimation can either be done in real time or later. For space applications, this opens up the flexibility for satellite engineers to decide whether to execute signal processing and position estimation only after the data downlink on ground (Option A), whether signal processing shall be done onboard and position estimation on ground (Option B), or finally, whether all three tasks shall be executed onboard as for most traditional GNSS receivers (Option C). These choices imply the opportunity to trade onboard processing effort and power versus downlink capacity. This aspect will be further addressed in Section 3.3.

The short sampling times however have their drawbacks. First, as the signal transmission time from the GNSS satellite cannot be decoded, initial estimates of position and time may be required or techniques such as Coarse Time Positioning may need to be applied (Van Dierendonck et al., 2018). In addition, the ephemeris of the GNSS satellites cannot be decoded during this short sampling interval. Thus, this information has be to provided externally.

A high-level onboard GNSS snapshot receiver architecture is shown in Fig. 4. Here, the received signals from the antenna are provided to the RF frontend for signal capturing, which complies the functions of down conversion and

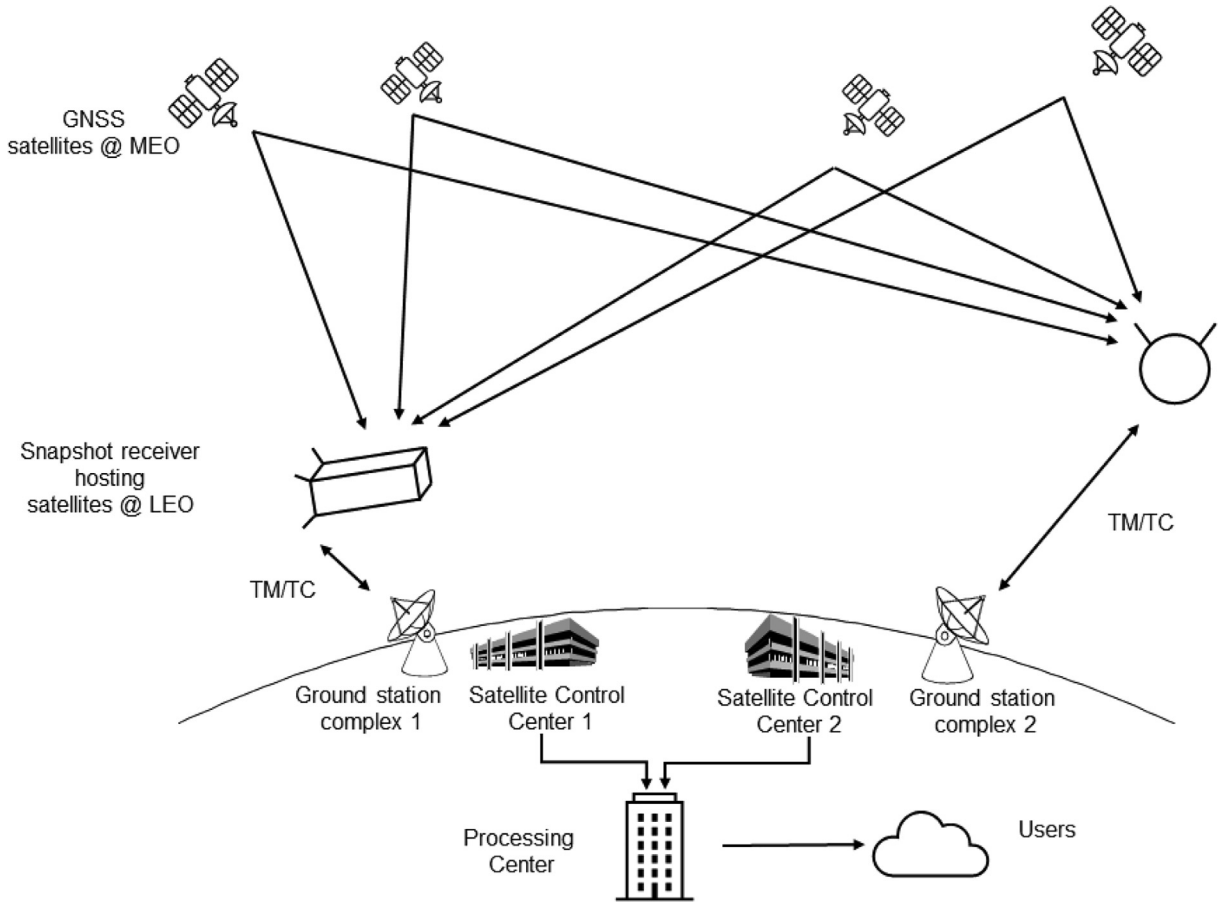

Fig. 3. Concept of Operations of an architecture to provide updated atmospheric models using a LEO space segment of diverse satellites hosting snapshot GNSS receivers (TM: Telemetry, TC: Telecommand).

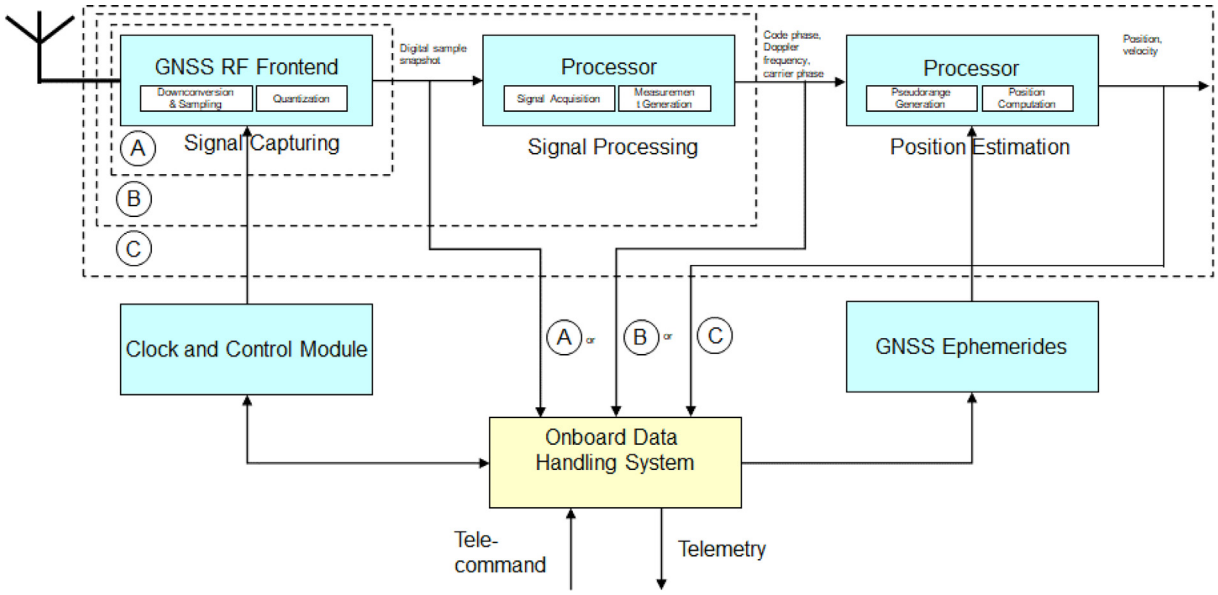

Fig. 4. High-level GNSS snapshot receiver architecture. From the options A, B, or C, the systems engineer will select one, according to the spacecraft characteristics and constraints.

sampling as well as quantization. There are three options indicated. Option A will provide the digital sample snapshot to the Onboard Data Handling System (OBDHS) for downlink via telemetry. This is option with the least power requirements and the highest requirements for downlink volume. Option B would use the digital sample snapshot for onboard signal processing to derive the measurements. This requires additional processing and thus power, but greatly reduces the downlink budget as compared to Option A. Option C would further perform pseudorange generation and position estimation onboard. This option is most efficient for downlink capacity but requires the most onboard processing and thus onboard power usage.

Telecommands will be required to control the GNSS snapshot receiver and provide timing signals as to when the snapshot shall be taken. If Option C is chosen for, broadcast ephemeris information will need to be uplinked to the spacecraft to allow position estimation.

3. Detailed characterization and performance analysis

This Section describes sample GNSS snapshot hardware, that is a exemplary for its hardware components and its characteristics in terms of its SWaP-C characteristics and its impact on key subsatellite systems.

3.1. GNSS characteristics

As an example of a terrestrial Snapshot GNSS receiver, we base our considerations on the SNAPPERGPS, a receiver developed at the University of Oxford (Beuchert and Rogers, 2021). The SNAPPERGPS is based on fast and reliable algorithms, provided as open implementation, that uses time periods of the signal of 12 milli-seconds that are sampled at 4 MHz and quantized with a single bit per second. The receiver achieves a reliability of 97 % and delivers positions of 11 m median horizontal accuracy. For space applications, the expected 3D position error, based on the fact that the Vertical Dilution of Precision (VDOP) will be higher than the Horizontal Dilution of Precision (HDOP), is $\sim \sqrt{3} * 11\,\mathrm{m} = 19\,\mathrm{m}$.

The hardware components of the SNAPPERGPS receiver are a Skyworks SE4150L integrated GPS receiver circuit, a SILICON LABS EFM32HG310F64 microcontroller with an ARM Cortex-M0+ core and a USB interface, and a 512 Mbit serial NAND flash memory IC (Beuchert and Rogers, 2021). For terrestrial applications, the receiver is combined with a battery (e.g. LP401528) and an antenna (e.g. SIRETTA ECHO 27) which allows to acquire one position per hour over a year (Beuchert and Rogers, 2021).

The total net size of the three ICs is estimated to be around 8x8 mm^2 without antenna which will have a net mass of 0.3 gr. For terrestrial applications, based on this Commercial Off The Shelf (COTS) approach, the total cost of such package is ~14 US$ based on a batch size of 100. Of course, as explained in Section 4, the cost of space qualification efforts are orders of magnitude larger, even for technology demonstration purposes.

3.2. Power budget

Based on Beuchert and Rogers (2021) and assuming a voltage level of 3.7 V, the average power consumption of the microcontroller in sleeping mode is 5.3 μW. Each snapshot requires a total energy of 1.0 μWh. Taking the average power consumption of the SIRETTA ECHO 27 antenna as benchmark, we will use 37 mW as value for the power consumption for the antenna. Fig. 5 shows the power consumption of the receiver ICs as a function of the sampling times 60 s, 600 s, 1 hr, 1 orbital period, 1 day, respectively.

3.3. 3.3.OBDH budget

As explained in Section 2.4, there are three options to store snapshot data onboard the satellite before transmitting them to ground, namely as digital sample, as measurements or as position information. Based on a snap duration of 12 ms and a sampling of 4.092 MHz with a 2-bit amplitude quantisation, a total of 49,104 samples of 2 bits would be recorded, i.e. 98 kb as digital sample (Option A). Assuming that 10 satellites would be visible from the constellations GPS, Galileo, and BeiDou and using a single frequency receiver, a total of 10 code phases (stored as 4-Byte value) would result from signal processing. If we would use in addition Signal-to-Noise ratios (stored as 1-Byte value), we would result in 400 bits per sample, without time tags (Option B). Finally, if we would only use position fixes, we would need a total of 256 bits including the time tag (Option C).

Table 1 lists typical data storage requirements for the GNSS snapshot receiver based on the three options for various data sampling frequencies.

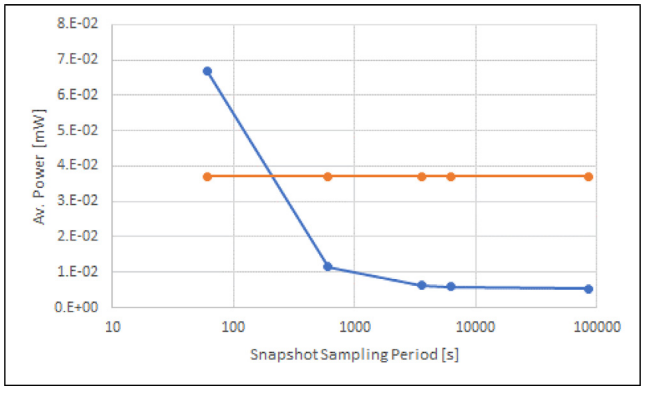

Fig. 5. Average power consumption of a sample snapshot receiver (blue line: ICs, orange line: antenna) as a function of the snapshot sampling period. The shown IC's power consumption refers to Option A (signal capturing) only.

Table 1
Data sizes [bit] for daily operations of the three options, depending on the snapshot sampling period (60 s, 600 s, 1 h, 1 orbital revolution).

Options	Single snap	60 s/d	600 s/d	1 h/d	1 orb./d
A (digital sample)	9.82E+04	1.41E+08	1.41E+07	3.26E+06	1.68E+06
B (measurements)	4.00E+02	5.76E+05	5.76E+04	1.33E+04	6.86E+03
C (position fix)	2.56E+02	3.69E+05	3.69E+04	8.51E+03	4.39E+03

3.4. Link budget

It is instructive to assess what the impact of the accumulated data volume from a snapshot GNSS receiver would be on the downlink budget for spacecraft. Let us assume a LEO satellite at 350 km altitude having a downlink frequency of 435 MHz. If we further assume an extremely miniaturized, highly power-constrained spacecraft, such as the Delfi-PQ PocketCube satellite with a form factor of 5 × 5 × 15 cm (Delfi-PQ, 2023) and a transmit power of 0.25 W, it would be possible to have a data rate of 4 kb/s and still achieve at positive link margin at 5° elevation. For a pass duration of about 10 min, this would allow to downlink about 2.4 Mb per pass.

Assuming that not more than one pass per day would be available for payload data downlink, this implies, that even extremely small PocketCube satellites could support Snapshot GNSS receiver operations in Option B and in Option C for all snapshot sampling periods shown in Tab. 1. Triple-unit CubeSats could support sampling periods of Option A, shown in Tab. 1 of snapshot data once per orbit (Option A) and possibly of once per hour. If engineers would choose to reduce onboard processing to the maximum extent and prefer to downlink digital samples even for high sampling frequencies instead, the use of microsatellites may be necessary.

4. Roadmap towards implementation

The previous Sections have shown the potential of using GNSS snapshot receivers for spaceborne applications in a flexible and highly efficient way, based on their low SWaP-C values. An example of applications are science purposes, such as thermospheric neutral density estimates to improve SSA. However, there is still a long way before their demonstration in space or even their operational usage based on a distributed space segment. Still, their potential is already recognized by space agencies, e.g. the European Space Agency (ESA) with its Advancing Positioning Navigation and Timing (navisp) program [https://navisp.esa.int/]. Currently, the Technology Readiness Level (TRL) of modern GNSS snapshot receivers for space applications is estimated to be in a range of 2–4. This Section aims at sketching a roadmap towards their operational usage and provides key steps to increase their TRLs.

First, while GNSS snapshot receivers are nowadays exclusively used for terrestrial applications, their on-ground characterization for intended spaceborne applications needs to be planned, prepared, performed, analyzed and documented. Specific aspects in this regard comprise their performance with respect the specific conditions in space, such as high dynamics and initialization. To this end, specific algorithms will need to be developed, both for the receiver itself as well as for the specific science application.

Second, detailed architectures for the onboard implementation of such systems need to be developed, based on the generic concepts that have been introduced in Section 3. Such architectures will typically be derived based on science and mission requirements in a top-down manner. However, as the receiver offers such low SWaP-C values, a bottom-up technology demonstration approach appears more efficient which makes use of their demonstration on femto-, pico- or nano-satellites, before embarking on micro- or even larger satellites. Also, the risk position based on the opportunities offered by such low-cost systems needs to be carefully analyzed to trade extensive testing programs versus redundancy concepts.

Next, snapshot receiver developments for space applications need to be enabled through research and development programs on national or international level, which allow for proper test and validation programs. These include standard mechanical, thermal and radiation test activities as well as associated stress testing.

Early-on in the roadmap, and long before a prototype and flight demonstration can be considered, programmatic questions need to be addressed and clarified, such as legal and regulatory aspects. These questions are, e.g., related to the Wassenaar Arrangement established in 1996 and being a successor of the Coordinating Committee for Multilateral Export Controls (CoCom). Even though snapshot GNSS receivers will operate at the designated L- and E-Band frequencies, their usage for space applications will still need to be investigated.

Next, the development of space-capable engineering (EM) and flight models (FM) of GNSS snapshot receivers needs to be pushed along with the development of technology demonstration missions. Given the low SWaP-C values, it appears to be most efficient to operate those FMs on femto-, pico- or nano-satellites first, or to use them on small micro-satellites for demonstration, characterization and validation. The exemplary use of snapshot GNSS receivers for niche science applications, such as atmospheric neutral density estimation and model improvements, should best be linked to such flight demonstrations.

Finally, concepts for the operational implementation and usage of spaceborne snapshot GNSS receivers need

to be developed. This can comprise single or multiple satellites, such as flying in a constellation to provide the best coverage and spatial and temporal resolution as required by scientists. Again, given the low SWaP-C of these sensors, innovative concepts, like using them as hosted payloads on space missions, or even establishing a System of Systems (SoS) of missions utilizing such receivers, may be considered.

5. Conclusion and recommendations

This paper proposed the use of spaceborne snapshot GNSS receivers for scientific applications, in particular the estimation of neutral thermospheric density and its associated models for improved space situational awareness. Various methods to retrieve such density estimates from GNSS receivers have been reviewed and it was shown that snapshot GNSS receivers provide an position accuracy about a factor of 100 superior to TLEs. For a snapshot sampling period of 8 h, snapshot GNSS receivers provide a relative density accuracy comparable to TLEs or high-grade geodetic GNSS receivers, improving largely the time update rate of density values from TLEs of three days. A very attractive opportunity for using spaceborne snapshot GNSS receivers for scientific applications stems from their low SWaP-C values, which makes their use in a Distributed Space System, which can comprise heterogenous satellites, highly beneficial and will improve the density corrections further by a factor of $\sqrt{N}$ with N being the number of satellites in the system. The onboard architecture for snapshot GNSS receivers has been developed with a focus on the trade space of onboard processing versus downlink data volume. The impact of using spaceborne snapshot GNSS receivers for critical subsystems, such as the power, onboard data handling and communication subsystems and their respective trade spaces, has been assessed. It was shown that niche science can even be realized flying snapshot GNSS receivers on pico-satellites, such as PocketCubes, in the future. Finally, a roadmap has been sketched to show how the realization of spaceborne snapshot GNSS receivers, including existing challenges, for scientific applications can be pursued.

Declaration of competing interest

The authors declare that they have no known competing financial interests or personal relationships that could have appeared to influence the work reported in this paper.

Acknowledgement

The research leading to this publication has to a great extent been performed as part of the 2023 Byram Distinguished Visiting Professorship at the Ann and H.J. Smead Department of Aerospace Engineering Sciences at the University of Colorado Boulder, University of Colorado, Boulder, CO, USA. The first author is grateful to all faculty of the department, enabling and supporting his research stay and for the hospitality, he experienced.

References

Aida, S., Patzelt, T., Leushacke, L., Kirschner, M.D., Kiehling, R., 2009. Monitoring and Mitigation of Close Proximities in Low Earth Orbit. In: Proceedings of the 21st International Symposium on Space Flight Dynamics, ISSFD 2009.

Arnold, D., Montenbruck, O., Hackel, S., 2019. Satellite laser ranging to low Earth orbiters: orbit and network validation. J. Geod. 93, 2315–2334. https://doi.org/10.1007/s00190-018-1140-4.

Behzadpour, S., Mayer-Gürr, T., Krauss, S., 2021. GRACE Follow-On accelerometer data recovery. J. Geophys. Res.: Solid Earth 126. https://doi.org/10.1029/2020JB021297 e2020JB021297.

Beuchert, J., Rogers, A., 2021. "SnapperGPS – Algorithms for Energy-Efficient Low-Cost Location Estimation Using GNSS Signal Snapshots. In: Proceedings of the 19th ACM conference on Embedded Networked Sensor Systems (SenSys'21), Coimbra Portugal. https://doi.org/10.1145/3485730.3485931.

Brandt, D.A., Bussy-Virat, C.D., Ridley, A.J., 2020. A simple method for correcting empirical model densities during geomagnetic storms using satellite orbit data. Space Weather 18. https://doi.org/10.1029/2020SW002565.

Bruinsma, S., Thuillier, G., Barlier, F., 2003. The DTM-2000 empirical thermosphere model with new data assimilation and constraints at lower boundary: Accuracy and properties. J. Atmos. Sol. Terr. Phys. 65, 1053–1070. https://doi.org/10.1016/S1364-6826(03)00137-8.

Cicalo, S., Beck J., Minisci E., Guerra, F., Holbrough, I., Lemmens, S., Riccardi, A., Vasile, M., 2017. GOCE RADAR-BASED ORBIT DETERMINATION FOR RE-ENTRY PREDICTIONS AND COMPARISON WITH GPS-BASED POD. In: Proc. 7th European Conference on Space Debris, Darmstadt, Germany, 18–21 April 2017, paper # 317, published by the ESA Space Debris Office, Ed. T. Flohrer & F. Schmitz, (https://conference.sdo.esoc.esa.int/proceedings/sdc7/paper/315/SDC7-paper315.pdf).

Delfi-PQ, 2023. Delft University of Technology, https://www.tudelft.nl/lr/delfi-space/delfi-pq [Online]. Last accessed 2023/06/12.

Doornbos, E., Klinkrad, H., Visser, P., 2008. Use of two-line element data for thermosphere neutral density model calibration. Adv. Space Res. 41 (7), 1115–1122. https://doi.org/10.1016/j.asr.2006.12.025.

Friis-Christensen, E., Lühr, H., Knudsen, D., Haagmans, R., 2008. Swarm – An Earth Observation Mission investigating Geospace. Adv. Space Res. 41 (1), 210–216. https://doi.org/10.1016/j.asr.2006.10.008.

Gill, E., Morton, J., Axelrad, P., Akos, D.M., Centrella, M., Speretta, S., 2023. Overview of space-capable global navigation satellite systems receivers: heritage, status and the trend towards miniaturization. Sensors 23, 7648. https://doi.org/10.3390/s23177648.

Granholm, G.R., Proulx, R.J., Cefola, P.J., 2002. Requirements for accurate near-real time atmospheric density correction. J. Astronaut. Sci. 50, 71–97. https://doi.org/10.1007/BF03546331.

Hoots, F., Roehrich, R., 1980. Spacetrack report no. 3: Models for propagation of NORAD element sets. Tech. rep., Aerospace Defense Center, Peterson Air Force Base. https://doi.org/10.21236/ADA093554.

Jacchia, L.G., 1979. CIRA 1972, recent atmospheric models, and improvements in progress. In: Proceedings of the Open Meetings of the Working Groups on Physical Sciences of the Twenty-First Plenary Meeting of COSPAR, Innsbruck, Austria, 29 May - 10 June 1978, 179–192. https://doi.org/10.1016/B978-0-08-023417-5.50032-6.

King-Hele, D., 1987. Satellite Orbits in an Atmosphere: Theory and Applications. Blackie, Glasgow.

Kuang, S., Desai, A., Sibthorpe, X Pi, 2014. Measuring atmospheric density using GPS–LEO tracking data. Adv. Space Res. 53 (2), 243–256. https://doi.org/10.1016/j.asr.2013.11.022.

Landerer, F., Flechtner, F., Save, H., Webb, F., Bandikova, T., Bertiger, W., Bettadpur, S., Byun, S., Dahle, C.h., Dobslaw, H., Fahnestock, E., Harvey, N., Kang, Z., Kruizinga, G., Loomis, B., McCullough, C.h., Murböck, M., Nagel, P., Paik, M., Yuan, D.N., 2020. Extending the global mass change data record: GRACE follow-on instrument and science data performance. Geophys. Res. Lett. 47 (12). https://doi.org/10.1029/2020GL088306.

Marcos, F.A., Bowman, B.R., Sheehan, R.E., 2006. Accuracy of Earth's Thermospheric Neutral Density Models. In: AIAA/AAS Astrodynamics Specialist Conference, Keystone, CO, USA, August 2006. https://doi.org/10.2514/6.2006-6167.

Montenbruck, O., Gill, E., 2001. Satellite Orbits: Models, Methods and Applications, Springer. https://doi.org/10.1007/978-3-642-58351-3.

Moore, P., Turner, J.F., Qiang, Z., 2003. CHAMP orbit determination and gravity field recovery. Adv. Space Res. 31 (8), 1897–1903. https://doi.org/10.1016/S0273-1177(03)00164-9.

Nicholas, A.C., Gilbreath, G.C. Thonnard S.E., et al., 2003. The Atmospheric Neutral Density Experiment (ANDE) and Modulating Retroreflector in Space (MODRAS): combined flight experiments for the space test program, in Proceedings Volume 4884, Optics in Atmospheric Propagation and Adaptive Systems V, Crete, Greece, March 2003. https://doi.org/10.1117/12.462642.

Picone, J.M., Hedin, A.E., Drob, D.P., Aikin, A.C., 2002. NRLMSISE-00 empirical model of the atmosphere: Statistical comparisons and scientific issues. J. Geophys. Res. 107, 1468. https://doi.org/10.1029/2002JA009430.

Picone, J.M., Emmert, J.T., Lean, J.L., 2005. Thermospheric densities derived from spacecraft orbits: Accurate processing of two-line element sets. J. Geophys. Res. 110, A03301. https://doi.org/10.1029/2004JA010585.

Pilinski, M.D., Palo, S.E., 2009. An innovative method for measuring drag on small satellites. In: 23th Annual AAIA/USU Conference on Small Satellite, Logan, Utah, 2009.

Powell, T.D., Martzen, P.D., Sedlacek, S.B., Chao, C.-C., Silva, R., Brown, A., Belle, G., 1999. GPS Signals in a Geosynchronous Transfer Orbit: "Falcon Gold" Data Processing. In: Proceedings of the 1999 National Technical Meeting of The Institute of Navigation, San Diego, CA, January 1999, pp. 575–585.

Reigber, Ch., Lühr, H., Schwintzer, P., 2002. CHAMP mission status. Adv. Space Res. 30 (2), 129–134. https://doi.org/10.1016/S0273-1177(02)00276-4.

Rummel, R., Horwath, M., Yi, W., Albertella, A., Bosch, W., Haagmans, R., 2011. GOCE, Satellite Gravimetry and Antarctic Mass Transports. Surv. Geophys. 32, 643–657. https://doi.org/10.1007/s10712-011-9115-5.

Siemes, C., de Teixeira da Encarnação, J., Doornbos, E., van den Ijssel, J., Kraus, J., Pereštý, R., Grunwaldt, L., Apelbaum, G., Flury, J., Olsen, P.E.H., 2016. Swarm accelerometer data processing from raw accelerations to thermospheric neutral densities. Earth Planets Space, 68–92. https://doi.org/10.1186/s40623-016-0474-5.

Srinivasan, J., Bar-Sever, Y., Bertiger, W., Lichten, S., Muellerschoen, R., Munson, T., Spitzmesser, D., Tien, J., Wu, S.-C., Young, L., 2000. microGPS: On-orbit demonstration of a new approach to GPS for space applications. Navigation: J. Instit. Navig. 47, 121–127. https://doi.org/10.1002/j.2161-4296.2000.tb00207.x.

Tapley, B., Bettadpur, S., Watkins, M., Reigber, C.h., 2004. The gravity recovery and climate experiment: Mission overview and early results. Geophys. Res. Lett. 31 (9). https://doi.org/10.1029/2004GL019920.

Teunissen, P.J.G., Montenbruck, O., 2017. Global Navigation Satellite Systems. Springer Handbook. https://doi.org/10.1007/978-3-319-42928-1.

USSTRATCOM, 2023. "SPACE-TRACK.org," Joint Force Space Component Commander/J3, [Online]. Available: https://www.space-track.org. [Accessed 2023/06/01].

van den Ijssel, J., Visser, P., 2007. Performance of GPS-based accelerometry: CHAMP and GRACE. Adv. Space Res. 39 (10), 1597–1603. https://doi.org/10.1016/j.asr.2006.12.027.

van den IJssel, J., Doornbos, E., Iorfida, E., March, G., Siemes, C., Montenbruck, O., 2020. Thermosphere densities derived from Swarm GPS observations. Adv. Space Res. 65 (7), 1758–1771. https://doi.org/10.1016/j.asr.2020.01.004.

Van Dierendonck, K., Al-Fanek, O., Petovello, M., 2018. What Is Snapshot Positioning and What Advantages Does It Offer?, InsideGNSS, December 6, 2018. https://insidegnss.com/what-is-snapshot-positioning-and-what-advantages-does-it-offer/ (last accessed 2023/06/08).

Visser, P.N.A., IJssel, J.A.A.V.D., 2016. Calibration and validation of individual GOCE accelerometers by precise orbit determination. J. Geod. 90, 1–13. https://doi.org/10.1007/s00190-015-0850-0.

Wang, M., Qin, H., Jin, T., 2019. Massive terminal positioning system with snapshot positioning technique. GPS Solut. 23, 31. https://doi.org/10.1007/s10291-018-0821-z.

Willis, P., Deleflie, F., Barlier, F., Bar-Sever, Y.E., Romans, L.J., 2005. Effects of thermosphere total density perturbations on LEO orbits during severe geomagnetic conditions (Oct–Nov 2003) using DORIS and SLR data. Adv. Space Res. 36 (3), 522–533. https://doi.org/10.1016/j.asr.2005.03.029.

Zhao, Z., Wang, Z., Zhang, Y., 2019. A spherical micro satellite design and detection method for upper atmospheric density estimation. Int. J. Aerosp. Eng. https://doi.org/10.1155/2019/1758956.